ISSN 0010-9525, Cosmic Research, 2015, Vol. 53, No. 6, pp. 423–429. © Pleiades Publishing, Ltd., 2015.
Original Russian Text © M.I. Panasyuk, M.V. Podzolko, A.S. Kovtyukh, I.A. Brilkov, N.A. Vlasova, V.V. Kalegaev, V.I. Osedlo, V.I. Tulupov, I.V. Yashin, 2015, published in Kosmicheskie Issledovaniya, 2015, Vol. 53, No. 6, pp. 461–468.

Operational Radiation Monitoring in Near-Earth Space Based on the System of Multiple Small Satellites

M. I. Panasyuk, M. V. Podzolko, A. S. Kovtyukh, I. A. Brilkov, N. A. Vlasova, V. V. Kalegaev, V. I. Osedlo, V. I. Tulupov, and I. V. Yashin

Skobeltsyn Institute of Nuclear Physics, Moscow State University (SINP MSU), Moscow, Russia

e-mail: ikt0840@mail.ru

Received February 6, 2015

Abstract—The operational monitoring of radiation conditions in different orbits in near-Earth space is crucial for ensuring the radiation safety of space flights. The intensity of ionizing radiation fluxes in near-Earth space varies within several orders of magnitude. Therefore, existing averaged empirical models cannot always be used to estimate specific radiation conditions in orbits. The forecast of solar cosmic rays is even less reliable. This paper presents a version of the global system of radiation monitoring in near-Earth space based on the system of multiple small satellites. The considered system of satellites with identical radiometric equipment will provide operational information on the fluxes of electrons and protons of Earth radiation belts and solar cosmic rays, which will make it possible to create 3D pictures of the distribution of particle fluxes in real time.

DOI: 10.1134/S0010952515060039

INTRODUCTION

The study of fluxes of charged particles in space is one of the most important tasks in space research, and it is extremely relevant both in terms of learning the laws of generation and spatiotemporal variations of such fluxes and from the point of view of determining the radiation conditions of various materials used in spacecraft (SC) design. According to existing expert estimates, more than half of the failures of systems onboard SCs occur because of adverse effects of the surrounding space environment on the materials and units of SC equipment with the main role played by different types of radiation exposure [1].

Information about the radiation environment is extremely important for the development of predictive models of space weather and climate, support of sustainable and reliable space communications, and improvement of the accuracy of global navigation and positioning systems.

Currently, models of the spatial–energetic distributions of fluxes of protons and electrons of the Earth radiation belts (ERB) for periods of maximum and minimum solar activity (SA) developed based on satellite measurements are used for the evaluation of radiation environment in orbits of artificial Earth satellites (AES). The most well-known are the models AP8 and AE8 [2, 3]. Experimental data from 24 AESs (of *Explorer*, *Injun*, *Telstar*, *IMP*, *OGO*, *Pegasus*, *ATS*, and other series) during the period from 1958 to 1978 were used in their development. It should be noted that most of the experimental data used in these models for the period of minimum SA refers to 1964 and for the maximum SA period, to 1970 for AP8 and to 1967 for AE8. Currently, new models AP9 and AE9 [4] based on the present experimental data are being developed.

ERB models [5–8] were also developed in SINP MSU that have been used as the basis for national standards [9–11] that regulate methods of the evaluation of radiation conditions of the AES flight.

However, actual fluxes of energetic charged particles in AES orbits can differ significantly from model values. The fact is that even in quiet conditions fluxes of particles experience quite significant long-term variations. For example, in the model AE8, the dose of radiation in the orbit of the AES GLONASS decreases from maximum to minimum SA within a factor of two. The maximum of the twenty third SA cycle was observed in 2000–2001. In [12], the results of measurements of the radiation dose at the AES GLONASS are given for nearly 4 years (December 2006–May 2010), and a comparative analysis of experimental data and data calculated by the model AE8 of radiation doses behind the shielding of ~2 g/cm^2 Al has been carried out. It is shown (see Fig. 2 in [12]) that there is a significant long-term reduction in the time series of 6-month averaged experimentally measured radiation doses in the outer radiation belt in the SA minimum of the twenty third cycle, but it differs from the predictions of the model by more than one order of magnitude.

Changes in the spatial distribution of ERB particle fluxes occur as a result of short-term magnetospheric disturbances. In [13], cases of the emergence of new belts of relativistic electrons with $E > 15$ MeV in the decay phase of magnetic storms are considered. Events were recorded at the AES *Cosmos-900* in 1977–1978 on magnetic shells $L = 3.2$–4.1. The values of recorded electron fluxes increased by several times compared to fluxes in a geomagnetically quiet time. The lifetime of electron belts associated with each magnetospheric disturbance was of the order of a week at altitudes of ~500 km. In the case of strong magnetospheric disturbances, a generation of belts able to exist for several weeks or even months was repeatedly recorded. A strong belt of protons and electrons with energies of tens of MeV in the region $L = 2–3$, which was formed after the sudden commencement of a strong magnetic storm on March 24, 1991, can be cited as an example. Fluxes of protons of the new belt with energies of >5...>100 MeV exceeded fluxes during the quiet time by two orders of magnitude and electrons with $E > 15$ MeV, by three orders of magnitude. This belt was found in experiments performed on the SC *CRRES* [14].

Finally, satellite measurements and the calculations of values of omnidirectional fluxes of particles based on them and used in the development of ERB models are quite complex. Therefore, model fluxes have some systematic error, at least within a factor of two.

Thus, we see that the real pattern of the fluxes of electrons and protons of the Earth radiation belt in AES orbits can differ significantly from that given by the existing ERB models. This also applies to other, even more irregular components of space radiation, such as solar cosmic rays (SCR).

Therefore, both empirical and mathematical models developed to date describing radiation fluxes averaged over many months and years do not reflect their variations and cannot always be used to evaluate the actual radiation conditions in AES orbits.

SYSTEM OF MULTIPLE SATELLITES. RADIATION MONITORING OPTION

The increase of the SC operating time and the use of components sensitive to ionizing radiation in their design put the need for monitoring of radiation conditions in SC orbits on the agenda. Based on experimental and theoretical data on ERBs, it can be shown that using radiation monitoring data obtained on specially selected orbits it is possible to predict radiation conditions for a large number of used orbits.

One option for this purpose is to develop a system of multiple satellites on specially selected orbits with identical radiometric equipment that will make it possible to receive data on the dynamics of the radiation fields differing in nature, energy, and composition of particles at different heights and reproduce three-dimensional patterns of the distribution of particle fluxes anywhere in the near-Earth space (NES) in real time.

The main objectives of the proposed system of AESs and the ground data processing center are (1) operational assessment of radiation levels, mainly from fluxes of electrons and protons of the ERB as well as from SCR protons used for a wide range of orbits, (2) testing and refinement of existing and development of new models of spatial–energetic distributions of the fluxes of electrons and protons of the ERB, and (3) acquisition of experimental data in order to solve the problems of the physics of the Earth's magnetosphere.

In the USSR, since 1960s work on the monitoring of cosmic radiation on the AES of *Electron*, *Prognoz*, *Molniya*, and *Cosmos* series has been carried out under the direction of Academician S.N. Vernov. Currently, SINP equipment for the measurement of charged particles is used on AESs of *Meteor* (low Earth-orbiting) and *Electro* (geostationary) series, as well as on GLONASS satellites.

The *NOAA* system, which has been operating since 1970, in which AESs *POES* and *GOES* are used for geophysical purposes at low polar orbits and geostationary orbit, respectively, should be noted among existing systems of multiple satellites for the monitoring of space radiation. The same equipment for the measurement of electrons and protons with energies from tens of keV to several hundred MeV, magnetic and electric fields and waves has been used in each of these AES series.

It should be noted that none of the existing satellite constellations fully solves the problem of the real-time monitoring of radiation conditions in the NES.

For the purposes of the radiation monitoring, it is proposed to use small spacecraft (SSC) as part of the system of multiple satellites. Over the past 20 years, technological advances in the miniaturization of electronic systems and reduction of their energy consumption have made it possible to develop and use more and more perfect SSC at a relatively low cost in the place of large satellite systems.

SSC effectiveness significantly depends on the features and parameters of their position control systems. In a broad class of scientific and practical problems solved at SSC high accuracy of their orientation and support of stabilization in orbital axes are not required. In this case, the basic requirements are the maximum simplicity and low manufacture cost, as well as minimal weight and power consumption. A magnitogyroscopic system of orientation and stabilization has these features. It is proposed to use such a system on SSC for the operational radiation monitoring.

ORBIT CONFIGURATIONS

L,B-coordinates are used to describe the spatial distribution of particle fluxes in radiation belts [15]. Parameter L for the dipole magnetic field is the distance from the center of the dipole to the top of the power line in the plane of the magnetic equator in Earth radii. It sets the drift shell of the particle motion. B is the magnetic field induction. Thus, the usual three-dimensional space is reduced to a two-dimensional one.

The task of the system of multiple SSC is to carry out operational measurements of particle fluxes at several points of each L-shell. For the remaining L-shell points, flux values can be calculated using the mea-

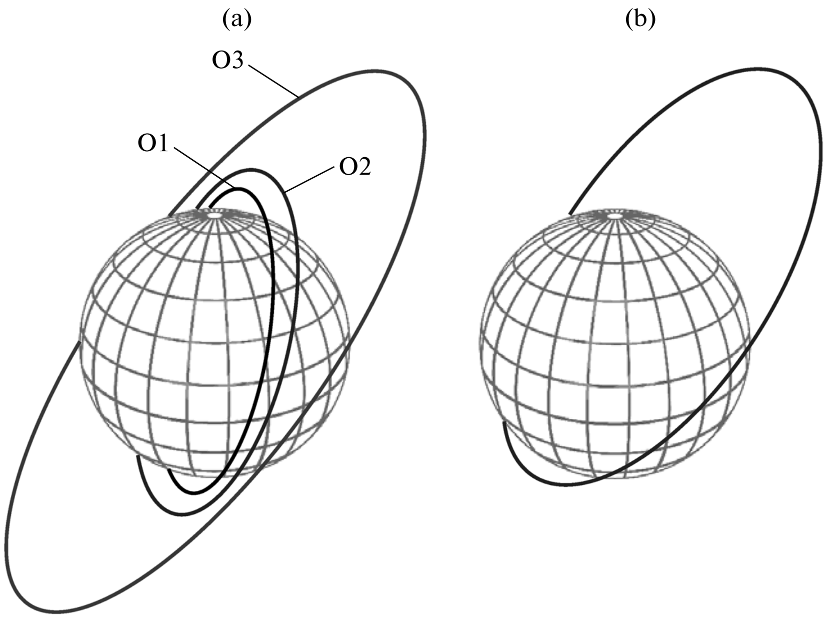

Fig. 1. Constellation options: three SSC in different circular orbits denoted as O1, O2, and O3 (a) and 2–3 SSC in the elliptical orbit (see text) (b).

surement data by the interpolation and extrapolation depending on the value of B (the "altitudinal variation") using known theoretical and empirical rules, and thus calculate fluxes for the arbitrary SC orbit.

Almost simultaneous intersection of the L-shell at several different points can be achieved by putting several SSC in different orbits. Figure 1a shows a version of the satellite constellation, which includes three spacecraft in circular orbits with altitudes 650, 1700, and 8000 km and inclinations of 80°, 77°, and 60°, respectively (O1, O2, and O3).

Figure 2 shows altitudinal variations of integral fluxes of electrons and protons calculated by models AE8/AP8, as well as areas in which said SSC orbits cross belts of electrons and protons on various L-shells. Altitudinal variations are constructed using geomagnetic field models IGRF.

The selection of orbits of SSC constellation is determined by characteristic features of altitudinal variations of ERB particle fluxes: (1) in the case of small B (up to heights of $h_{\min}(L, B) \sim 1000$ km) particle fluxes decrease with increasing B by the law close to power law, (2) for large values of B there is an exponential roll-off of the altitudinal variation, and (3) at altitudes ~1500–2000 km there is a narrow "intermediate" area.

Figure 2 shows that orbits O1, O2, and O3, intersect L-shells in the three above-mentioned areas with a different character of altitudinal variation. It is important for the interpolation accuracy of the altitudinal variation of fluxes.

In Fig. 1b, an elliptical orbit is shown, having perigee and apogee heights of 700 and 8000 km, perigee argument of 310°, inclination of 63.435°, and a period of ~3 hours as an alternative to the system of multiple SSC. The dotted line in Fig. 2 indicates the areas at which the orbit crosses radiation belts of electrons and protons on different L-shells. The graphs show that the orbit crosses all three above-mentioned areas, where there is a different character of the altitudinal variation of fluxes. For sufficient reliability of the constellation and frequency of measurements, it is advisable to put 2–3 AESs in elliptical orbits with the specified parameters but with different longitudes of the ascending node and at different phases of the orbital motion.

In this case, the elliptical orbit inclination is selected such that there is no drift of the argument of perigee because of differences between the Earth gravitational field and the central one. It requires high accuracy of setting the orbit inclination during the orbital injection within ~0.2°. Otherwise, the area of the L, B-space through which the orbit passes can be reduced significantly over the lifetime of AES.

Apparently, several successive measurements of the given L can be used for each SSC in calm and weakly disturbed geomagnetic conditions ($K_p < 3$). Since the SSC passes the whole range of longitudes in 12 hours, it will increase the statistics and, therefore, the approximation accuracy of the altitudinal variation.

MEASUREMENT OF OMNIDIRECTIONAL PARTICLE FLUXES

Omnidirectional measurements of ERB particle fluxes are required for the purposes of radiation monitoring. Since energy spectra, penetration capability, and radiation effects and electrization for the electrons

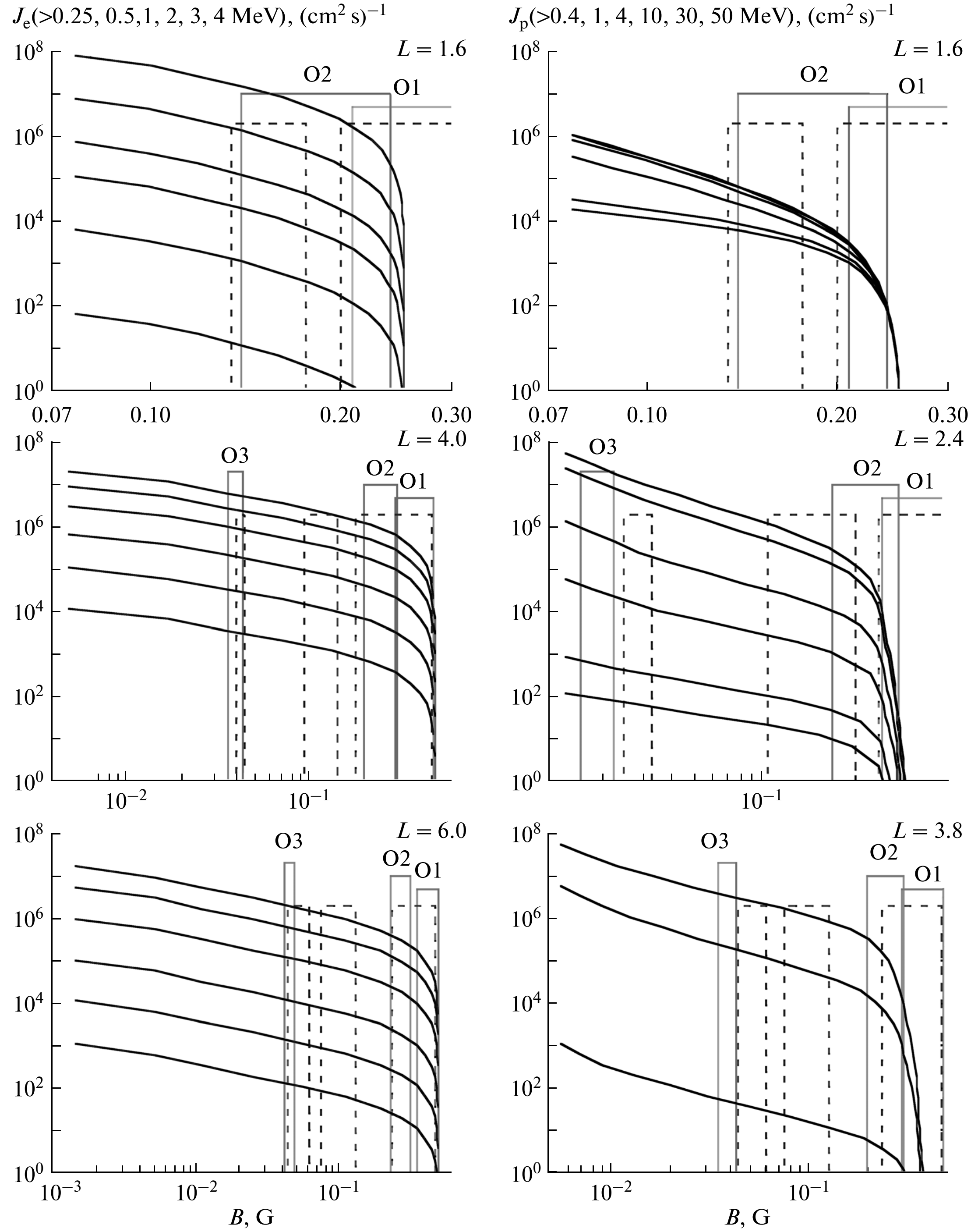

Fig. 2. Altitudinal variations of integral fluxes of electrons (left) and protons (right) by models AE8-max and AP8-max, respectively. Solid vertical lines show areas crossed by three circular orbits O1, O2, and O3, while dashed lines show those crossed by an elliptical orbit.

and protons associated with it are different, their fluxes should be measured separately.

However, the task of separate measurement of fluxes of electrons and protons of the ERB using a wide-angle detector with the field of view close to $\Omega = 2\pi$ is almost unsolvable. In this case, it is necessary to use multidirectional detectors, in which the particles are recorded within a relatively narrow aperture of the device. Such measurements can be used to calculate pitch-angle distribution of particle fluxes and the omnidirectional flux.

In our case, for a detector with the maximum possible field of view of 60° (i.e., 30° from the axis to the

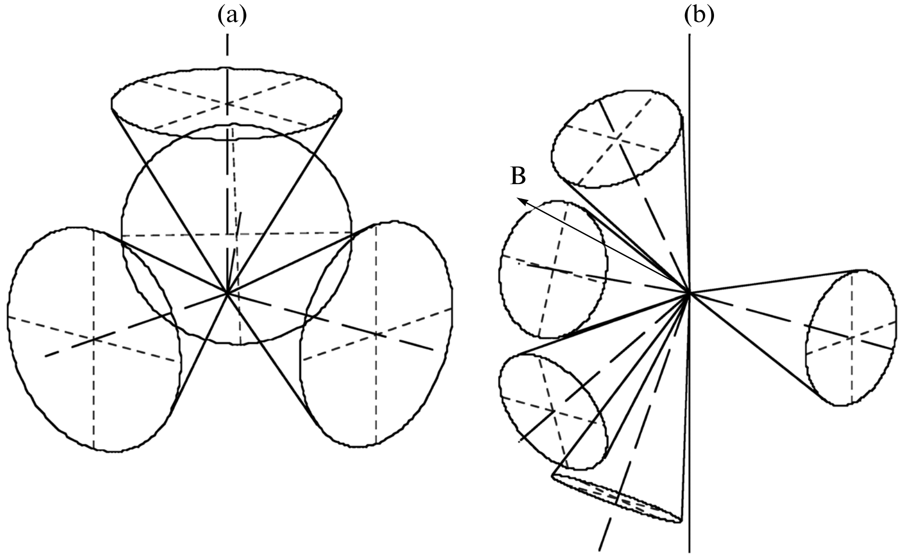

Fig. 3. Orientation options of detectors.

aperture cone generator), we have the following solid angle

$$\Omega_0 = 2\pi(1 - \sqrt{3}/2) = 0.268\pi.$$

For practical purposes, pitch angular distributions of ERB particles are well approximated by the function $j \propto \sin^A \alpha$, where j is the directed flux, α is the local pitch angle of the particles (the angle between vectors of the particle velocity and magnetic field at the measuring point), and $A(L, B, E)$ is the anisotropy parameter. For such pitch-angle distributions, the altitudinal variation of omnidirectional fluxes of particles with a given energy on the given L is as follows: $J \propto (B/B_0)^{-A/2}$, where B is the local value of the magnetic induction and B_0 is its value at the top of the force line (in the equatorial plane).

The magnitude A can take different values depending on energy and the type of particles, magnetic coordinates at the measurement point and the geomagnetic activity level.

For these pitch-angle distributions of particles, we obtain the following for the integral omnidirectional flux

$$J(>E) = \frac{4\pi}{A+1} j_0(>E),$$

where $j_0(>E)$ is the flux directed across the magnetic field, i.e., the flux of particles with $\alpha \sim 90°$.

If the axis of such a device is directed strictly along the local magnetic field vector, the particle flux within the device aperture of the field of view of 60° is $J_0(>E) \approx 0.5^{A+2} J(>E)$, if the device axis is angled at 45° to the local magnetic field vector, the flux of particles within the aperture of the device with a field of view of 60° is

$$J_{45}(>E) \approx \frac{(\sqrt{3}/2)^{A+1} - 0.5^{A+1}}{12} J(>E)$$

and if the axis of the device is directed strictly across the local magnetic field vector, the particle flux within the aperture of the device with a field of view of 60° is

$$J_{90}(>E) \approx \frac{1 - (\sqrt{3}/2)^{A+1}}{6} J(>E).$$

If we assume these fluxes to be average in all directions, then in order to obtain an omnidirectional flux they should be multiplied by (taking into account the limited aperture) by a factor of $4\pi/\Omega_0 = 14.925 \sim 15$.

Thus, for the device with the axis directed strictly along the local magnetic field vector, we obtain the following calculated integrated flux for A between 8 and 14:

$$J^*(>E) = \frac{4\pi}{\Omega_0} J_0 \approx kJ(>E),$$

where $k \sim (0.0002–0.06)$, i.e., the omnidirectional flux calculated by the readings of this device will be very low. Larger values of A considered in this case can be explained by the fact that the measurements along the field correspond to the area of the altitudinal variation roll-off (see Fig. 2).

For the device with an axis directed at an angle of 45° to the local magnetic field vector, for the values of A from 2 to 10 we obtain $k \sim (0.26–0.66)$; i.e., omnidirectional flux calculated by readings of this device will be significantly understated.

Finally, for a device with its axis directed strictly across the local magnetic field vector, for values of A from 2 to 10 we obtain $k \sim (0.88–2.0)$; i.e., omnidirectional fluxes calculated by readings of this device are the closest to actual values for typical values of A.

Therefore, for calculations of omnidirectional fluxes it is optimal to measure fluxes such that the axis of the field of view of at least one of the detectors on each SSC is directed across the magnetic field (or close to this direction). The three-component magnetometer on board of the spacecraft is a necessary condition to have the data on the orientation of the detectors. Recall that it is proposed to use a magnitogyroscopic system of orientation and stabilize on the SSC with orientation according to the magnetic field (at altitudes of 1000–8000 km its accuracy is not worse than 15°).

In the simplest case, a version of the device with four detectors at each SSC is preferable, where the axes of the fields of view of three of them are located along three axes of the rectangular Cartesian system and the axis of the fourth one, along the major axis of the cube built on axes of the first three (Fig. 3a). The angle between the axis of the fourth detector and the axes of each of the first three detectors is about ~55°, i.e., their apertures almost do not overlap. As a result we obtain of a "hedgehog" of detectors that almost completely covers one quadrant of the solid angle. It is desirable to direct the axis of one detector across the magnetic field.

In this arrangement of detectors, omnidirectional particle fluxes are calculated as follows: maximum for all four detectors values of the count rate at one point, referring to particles with local pitch angles close to 90° (the closer, the less anisotropy) are selected; these values are then divided by the geometric factor of the device and are multiplied by the factor of $4\pi(A + 1)^{-1}$. The value of the anisotropy index A is determined by data from all four detectors associated with data from magnetometers, which makes it possible to estimate the local pitch angles of particles and construct approximate pitch-angle distributions (or, roughly, by maximum and minimum values of the count rate in multidirectional detectors).

Figure 3b shows other detector orientation option schematically.

The version shown in Fig. 3b provides active three-axial SC orientation according to the magnetic field. In this version, the major axis of the AES (the vertical line in Fig. 3b), which has cylindrical form with solar panels on the side faces, is perpendicular to the equator plane. The main detector is always directed perpendicular to the local magnetic field vector and to the satellite major axis. It provides measurements for pitch angles ~90°. The axes of 3–4 detectors additional to the main ones lie in another semiplane composed of the local magnetic field vector and the major satellite axis. Together, they cover all the other pitch angles. The angle of view for all the detectors in this version is 35°.

RADIATION MONITORING EQUIPMENT

In order to carry out radiation monitoring in various orbits, the same equipment should be mounted on the SSC. It is proposed to use a spectrometer of protons and electrons (PES) as particle flux detector [16]. The equipment consists of several units of spectrometers and a general data processing unit. Structurally, spectrometer units can be implemented as separate units or they can be combined into a single housing.

The main element of the spectrometer is a unit with sensors consisting of several solid-state detectors with different thicknesses and a scintillation detector arranged one above the other on a common axis. Such detecting systems are widely used on AESs in devices intended for the detection of electrons and protons of the ERB as well as particles of SCR and GCR.

Energy ranges of detected particles (electrons of 0.15–10 MeV and protons from ~2 to >160 MeV) are divided into several intervals.

The separation of particles detected by the spectrometer on electrons and ions is carried by logic selection systems based on the principle of coincidence–anticoincidence of electrical impulses from various sensors constituting one spectrometer.

CONCLUSIONS

Measurements of cosmic radiation show a significant (by orders of magnitude) variations in fluxes of ionizing radiation because of solar activity and geomagnetic disturbances. However, available ERB models cannot always be used for the evaluation of specific radiation conditions of the SC operation.

In order to provide the monitoring of the radiation environment in the NES with the possibility to predict radiation conditions for SC in near-earth orbits, a complex of three specialized small spacecraft weighing less than 100 kg is proposed. Devices should be put into several circular orbits (with altitudes of 650, 1700, and 8000 km and inclinations of 80°, 77°, and 60°, respectively), where they will measure fluxes of energetic protons and electrons using several identical detector systems. An option with an elliptical orbit was also considered. SSC will be equipped with identical measuring equipment that comprises several multidirectional spectrometers of energetic electrons and protons (detectors) and the common data processing unit.

The proposed complex is designed to carry out real time distributions of particle fluxes, which will make it possible to accomplish operational monitoring tasks for these orbits and to estimate radiation doses anywhere in the NES in real time, i.e., for the other SC.

In addition to the solution of operational monitoring problems, the implementation of the proposed space system can contribute to the solution of other applied and scientific problems, such as: (1) testing and refinement of existing and development of new models of the spatial–energetic distribution of fluxes of energetic charged particles in the NES, and (2) obtaining of a large array of space-distributed homogeneous experimental data for the solution of problems of the Earth's magnetosphere physics.

ACKNOWLEDGMENTS

This work was supported by the Ministry of Education and Science of the Russian Federation, project no. RFMEFI60414X0127.

REFERENCES

1. Novikov, L.S. and Panasyuk, M.I., Studies of cosmic radiation and its impact on the materials and equipment of spacecrafts, *Vopr. At. Nauki Tekh., Ser.: Fiz. Radiats. Vozdeistv. Radioelektron. Appar.*, 2002, no. 4, pp. 3–13.
2. Sawyer, D.M. and Vette, J.I., AP-8 trapped proton environment for solar maximum and solar minimum, NSSDC/WDC-A-R&S 76-06, 1979.
3. Vette, J.I., The AE-8 trapped electron environment, NSSDC/WDC-A-R&S 1-24, 1991.
4. Ginet, G.P., O'Brien, T.P., Huston, S.L., et al., AE9, AP9 and SPM: New models for specifying the trapped energetic particle and space plasma environment, *Space Sci. Rev.*, 2013, vol. 179, nos. 1–4, pp. 579–615.
5. Panasyuk, M.I. Sosnovets, E.N., et al., The Earth's natural radiation belts, in *Model' kosmosa* (Cosmic Model), Moscow: MGU, 1983, vol. 3, pp. 66–91.
6. Panasyuk, M.I. and Sosnovets, E.N., Intensities of electrons and protons as a function of *L* and *B*, in *Model' kosmosa* (Cosmic Model), Moscow: MGU, 1983, vol. 3, pp. 421–531.
7. Getselev, I.V., Gusev, A.A., Darchieva, L.A., et al., Model' prostranstvenno-energeticheskogo raspredeleniya potokov zakhvachennykh chastits (protonov i elektronov) v radiatsionnykh poyasakh Zemli, (Model of the Spatial and Energy Distribution of Fluxes of Captured Particles (Protons and Electrons) in the Earth's Radiation Belts), Moscow: MGU, 1991.
8. Getselev, I.V., Sosnovets, E.N., Kovtyukh, A.S., et al., An empirical model of the radiation belt of helium nuclei, *Cosmic Res.*, 2005, vol. 43, no. 4, pp. 229–232.
9. GOST 25645.138-86. The Earth's Natural Radiation Belts. Model of Spatial and Energy Distribution of Proton Flux Density. Moscow, 1986.
10. GOST 25645.139-86. The Earth's Natural Radiation Belts. Model of Spatial and Energy Distribution of Electron Flux Density. Moscow, 1986.
11. OST 134-1044-2007. Hardware, Instrumentation, Facilities, and Equipment of Spacecrafts. Methods for calculation of radiation conditions on board space vehicles and determination of requirements on the resistence of space vehicle electronic radio equipment to naturally occurring charged particles in the cosmos. M.: Roscosmos, 2007.
12. Tverskaya, L.V., Balashov, S.V., Veden'kin, N.N., et al., Outer radiation belt of relativistic electrons during the minimum of the 23rd solar cycle, *Geomagn. Aeron. (Engl. Transl.)*, 2012, vol. 52, no. 6, pp. 740–745.
13. Gorchakov, E.V., Afanas'ev, V.G., Afanas'ev, K.G., et al., Study of fast charged particles using a Cherenko detector onboard the Kosmos-900 artificial earth satellite, *Izv. Vyssh. Uchebn. Zaved., Fiz.*, 1987, no. 10, pp. 69–74.
14. Mullen, E.G., Gussenhoven, M.S., Ray, K., and Violet, M.A., A double-peaked inner radiation belt: Cause and effect as seen on CRRES, *IEEE Trans. Nucl. Sci.*, 1991, vol. 38, pp. 1713–1718.
15. McIlwain C.E., Magnetic coordinates, *Space Sci. Rev.*, 1966, vol. 5, no. 5, pp. 565–584.
16. Getselev, I.V., Tulupov, V.I., and Shcherbovskii, B.Ya., An instrument for radiation control onboard spacecrafts, *Vopr. At. Nauki Tekh., Ser.: Fiz. Radiats. Vozdeistv. Radioelektron. Appar.*, 2006, nos. 3–4, pp. 89–91.

Translated by O. Pismenov